

# Optical Engineering

OpticalEngineering.SPIEDigitalLibrary.org

## **Wide-range tunability, thermal locking, and mode-crossing effects in Kerr optical frequency combs**

Guoping Lin  
Khaldoun Saleh  
Rémi Henriet  
Souleymane Diallo  
Romain Martinenghi  
Aurélien Coillet  
Yanne K. Chembo

**SPIE.**

# Wide-range tunability, thermal locking, and mode-crossing effects in Kerr optical frequency combs

Guoping Lin,\* Khaldoun Saleh, Rémi Henriet, Souleymane Diallo, Romain Martinenghi, Aurélien Coillet,<sup>†</sup> and Yanne K. Chembo

FEMTO-ST Institute [UMR6174], Optics Department, 16 Route de Gray, 25030 Besançon cedex, France

**Abstract.** We theoretically and experimentally investigate some effects related to the Kerr optical frequency comb generation, using a millimeter-size magnesium fluoride ultrahigh quality disk resonator. We show that the Kerr comb tunability can be extremely wide in the Turing pattern (or primary comb) regime, with an intermodal frequency that can be tuned from 4 to 229 multiple free spectral ranges (corresponding to a frequency spacing ranging from 24 GHz to 1.35 THz). We also discuss the role played by thermal locking while pumping the resonator, as well as the effect of modal crossing when broadband combs are generated. © 2014 Society of Photo-Optical Instrumentation Engineers (SPIE) [DOI: [10.1117/1.OE.53.12.122602](https://doi.org/10.1117/1.OE.53.12.122602)]

Keywords: whispering gallery mode resonators; Kerr combs; crystalline photonics; ultrahigh quality resonators.

Paper 140336SS received Feb. 28, 2014; revised manuscript received Jun. 4, 2014; accepted for publication Jun. 23, 2014; published online Jul. 14, 2014.

## 1 Introduction

Monolithic ultrahigh quality ( $Q$ ) factor optical resonators with small mode volumes have been used for the study of various nonlinear optical phenomena in the continuous-wave (CW) low pump power regime. Kerr nonlinearity-based hyperparametric oscillations have been investigated along that line.<sup>1,2</sup> The interplay of Kerr nonlinearity and group-velocity dispersion in these solid-state resonators further results in the formation of interesting optical frequency combs through a cascaded four-wave mixing process. Since the demonstration of the first extended Kerr frequency comb generation in an on-chip silica microtoroid resonator,<sup>3</sup> an intensive amount of work has been carried out to further understand this phenomenon. This interest has been driven by the fact that compared with mode-locked laser-based frequency combs, Kerr combs feature a compact size and consume less power.

Up to now, Kerr frequency combs have been demonstrated in various materials and resonator geometries. They usually include fused silica microtoroids,<sup>3,4</sup> microrods,<sup>5-7</sup> silica microdisks,<sup>8</sup> on-chip microring structures using high-index glass,<sup>9</sup> silicon nitride,<sup>10-15</sup> aluminum nitride,<sup>16</sup> and disk resonators made of magnesium fluoride<sup>12,17-22</sup> and calcium fluoride crystals.<sup>20,23-26</sup> The integrated high- $Q$  microring structure enables full chip-scale integration with waveguides. On the other hand, crystalline disk resonators can feature ultrahigh  $Q$  factors ( $>10^9$ ). Thus, they help to reduce the required pump power for comb generation, and they have the potential to produce low-phase noise microwave signals. Theoretically, better understanding of Kerr frequency combs has also been emerging. A modal expansion approach was recently derived,<sup>27,28</sup> and more recently, a normalized Lugiato-Lefever formalism has been applied on simulating microresonator-based Kerr combs.<sup>29-31</sup> As a result,

the formation of Turing patterns, solitons, and their stability analysis have been studied.<sup>19,32-34</sup>

From the application point of view, the potential application of Kerr frequency combs has been demonstrated in many fields, such as multiwavelength high-speed coherent data transmission with advanced modulation formats,<sup>13</sup> ultra-short pulse generation,<sup>15,22</sup> low-phase noise microwave generation,<sup>8,20,23</sup> and so on. Considering the stable and spectrally pure microwave signal, many advanced techniques have been recently applied for stabilizing combs, such as self-injection locking,<sup>7</sup> interleaved electro-optical comb stabilization,<sup>5,35</sup> Pound-Drever-Hall locking (PDH),<sup>20,23</sup> and atomic Rb transitions referencing.<sup>20</sup> However, many studies have shown that the formulation of full Kerr frequency combs may involve many stages and could feature multiple radio frequency (RF) beatnotes and relatively high phase noise.<sup>8,12,14</sup> Recently, studies propose that the initial stage of Kerr combs, the primary combs, or Turing patterns, is strongly phase-locked and could be ideal for a secondary frequency reference,<sup>21</sup> similar to hyperparametric oscillations.<sup>2,36</sup>

In this work, we investigate Kerr frequency comb generation in an overmoded MgF<sub>2</sub> whispering gallery mode (WGM) resonator. We achieve wide tunability in the Turing pattern regime when the resonator is pumped with fixed external pump power. We also discuss the thermal effects, as well as the asymmetric combs obtained owing to the influence of mode-crossing.

## 2 Experimental Setup

The experimental setup is illustrated schematically in Fig. 1. The WGM resonator used in this experiment is fabricated from a commercially available MgF<sub>2</sub> disk with a radius of ~6 mm. The disk is later centered and mounted on a home-made high-speed lathe. The edge of the disk is then carefully shaped and polished to create an optically smooth surface. The final disk features an intrinsic  $Q$  factor  $>10^9$  at 1550 nm. A tunable CW semiconductor laser with few

\*Address all correspondence to: Guoping Lin, E-mail: [guoping.lin@femto-st.fr](mailto:guoping.lin@femto-st.fr)

<sup>†</sup>Current address: NIST, Boulder, Colorado, United States

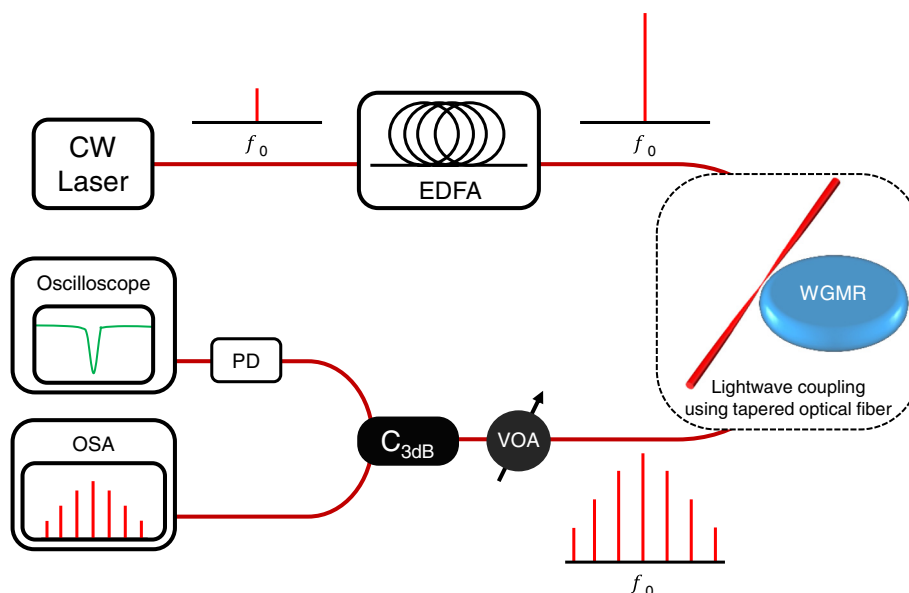


**Fig. 1** Schematic view of the experimental setup. EDFA, erbium-doped fiber amplifier; WGMR, MgF<sub>2</sub> whispering gallery mode resonator; PD, photodetector; OSA, high-resolution optical spectrum analyzer; VOA, variable optical attenuator; C<sub>3dB</sub>, 3 dB 1 × 2 optical coupler.

kilohertz spectral linewidth is used as a pump source. The laser power is then further amplified by an erbium-doped fiber amplifier. The final pump power can reach a few hundred milliwatts. In order to evanescently couple light in and out of the cavity, a fiber taper with a micrometer-size waist is used. The throughput of the fiber is then connected to a 3 dB 1 × 2 fiber coupler. The split output signals are monitored with a photodetector and a high-resolution optical spectrum analyzer (APEX 2440B) separately.

### 3 Results and Discussion

#### 3.1 Primary Combs with Spacing from Gigahertz to Terahertz

The formation of single free spectral range (FSR) Kerr combs could involve many stages and produces wide bandwidth and multiple RF beatnotes.<sup>8,12,14</sup> Recent theoretical work has also shown that chaotic behavior of Kerr combs<sup>27,37,38</sup> exists when the pumping is sufficiently high. Primary Kerr combs or Turing patterns, as the first stage of the full comb, shows a strong phase-locked behavior compared with other combs.<sup>21</sup> Experimentally, we demonstrate primary combs generation with 4-FSR, 44-FSR, and 229-FSR spacing in the same resonator. The corresponding frequencies are 23.7, 260.0, and 1351.0 GHz as shown in Fig. 2.

The theoretical model used to analyze comb generation here is a normalized Lugiato-Lefever equation with periodic boundary conditions<sup>30,32</sup>

$$\frac{\partial \psi}{\partial \tau} = -(1 + i\alpha)\psi + i|\psi|^2\psi - i\frac{\beta}{2}\frac{\partial^2 \psi}{\partial \theta^2} + F, \quad (1)$$

where  $\psi(\theta, \tau)$  is the total intracavity field in the moving frame,  $\theta \in [-\pi, \pi]$  is the azimuthal angle along the circumference of the disk, and  $\tau = \Delta\omega t/2$  is the dimensionless time, with  $\Delta\omega$  being the loaded mode linewidth. The dimensionless parameters in this equation are the frequency

detuning  $\alpha = -2(\omega_L - \omega_R)/\Delta\omega$ , which is the frequency detuning between the laser frequency  $\omega_L$  and the pumped mode resonance position  $\omega_R$ , the dispersion  $\beta = -2\zeta_2/\Delta\omega$ , with  $\zeta_2$  being the second-order Taylor coefficient of the eigenfrequency expansion and  $F^2$  being proportional to the external pump power.

In order to simulate similar primary combs, very different dispersion parameters are chosen for these three primary combs as shown in Fig. 2. It should be noted that the spectrum analyzer detects both the outcoupled intracavity field and the remaining pump field. This has to be taken into account when comparing the experimental and theoretical spectra. Although there are other different detuning and pump parameters to generate similar spectra, we believe that the main reason causing these significant different comb lines would be the various dispersion parameters in

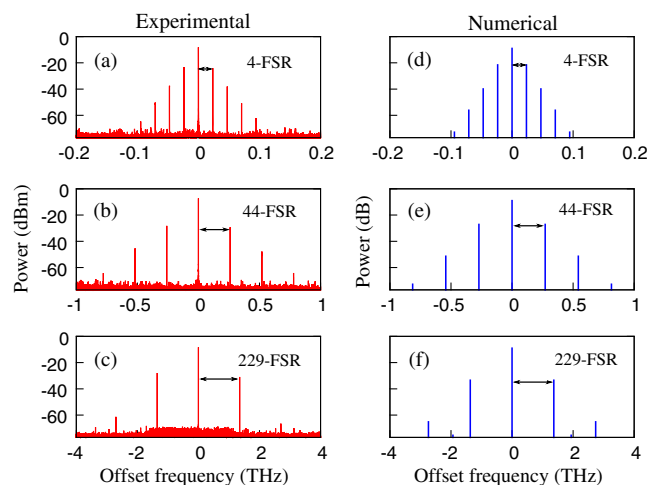


**Fig. 2** Left column: the experimentally obtained spectra for three different primary combs with 4-FSR, 44-FSR, and 229-FSR spacing, respectively (from top to bottom). Right column: The corresponding numerical simulation. 4-FSR:  $\alpha = -0.2$ ,  $\beta = 0.4$ ,  $F^2 = 6$ ; 44-FSR:  $\alpha = -1$ ,  $\beta = 0.003$ ,  $F^2 = 6$ ; 229-FSR:  $\alpha = -1.2$ ,  $\beta = 0.0012$ ,  $F^2 = 6$ .

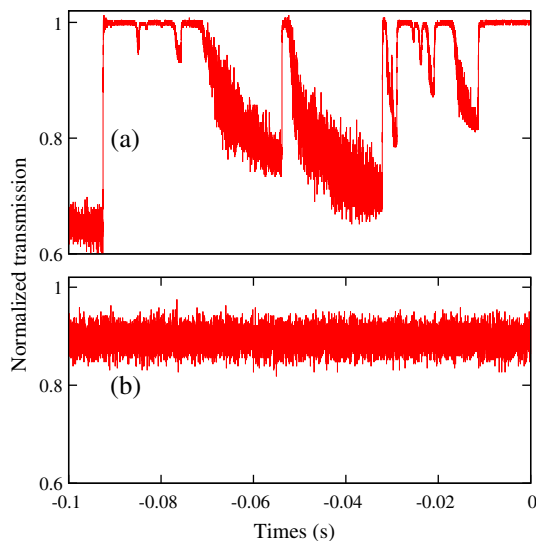


**Fig. 3** (a) Typical transmission spectrum with thermally broadened WGM resonances dips. The wavelength of the pump laser is increasing with time. (b) Transmission curve with fixed pump frequency where self-thermally stabilized state is achieved.

an overmoded resonator. These theoretical spectra are, however, in excellent agreement with those that can be obtained experimentally.

### 3.2 Thermal Noise and Kerr Combs

Figure 3(a) shows a typical thermally broadened WGM resonance spectrum in the throughput of the fiber taper. It results from the so-called thermal bistability in ultrahigh  $Q$  resonators.<sup>39</sup> In this experiment, the CW pump laser was detuned from the blue side of the resonances. Thus, the positive thermal coefficient of refractive index and thermal expansion then cause the red shift of the cold cavity resonance when it is continuously heated up by the pump laser. This feature has also been reported for the use of fast micro-laser characterization.<sup>40</sup> On the other hand, rich mode structures can be clearly seen in Fig. 3(a). It is expected that different families of modes feature different mode volumes,  $Q$  factors, and coupling efficiencies. As a result, they usually experience different thermal behaviors as shown in Fig. 3(a). There have been efforts to achieve single-mode ultrahigh  $Q$  WGM resonators.<sup>18,41</sup> However, this task proves to be very difficult.

As one can see, noise structures are observed on the blue side of the resonances. With increasing pump wavelength, the heating causes the shift of the resonance in the same direction. It slows down the relative detuning on the blue side of the resonance and makes the noise structure observable. On the red side of the resonance, the decreased coupled pump power no longer can overcome the heat dissipation. The temperature starts to decrease and, thus, the resonance shifts in the opposite direction of the laser scan, which leads to a strongly reduced scan time for this side. It should be noted that these noises are easily missed when advance functions like averaging or high resolution in the oscilloscope are used. Noises have been seen even without Kerr comb generation as shown in Fig. 3(b). When the pump laser is coupled into an optical resonance with a very narrow linewidth, a small relative frequency fluctuation between the

pump and the resonance frequency will be transformed into the amplitude noise and can be easily observed. Pump laser power, frequency, and cavity resonance jitter can result in this noise. The latter one is usually related to the fluctuation of the environmental temperature, the heating, and the Kerr shift induced by the absorbed pump laser. These fluctuations can be substantially attenuated using well-known laser-locking techniques.

An example of the thermal noise in the transmission spectrum with fixed pump frequency is shown in Fig. 3(b). We manually decrease the frequency of the pump laser until a WGM is excited, symbolized by a clearly increased noise amplitude. In each step, we need to wait a few seconds for the diffusive cooling and laser heating to reach an equilibrium. This timing depends on the disk size,  $Q$  factors, and the detuning step. Beside the eventual chaotic characteristics of the comb,<sup>27,37,38</sup> we believe that the thermal noise shown here is one of the main reasons why RF beatnote linewidths are of the order of (sub-)megahertz level when using free running pump laser with the self-thermally locking technique. However, this problem can be overcome by using PDH technique to lock the pump laser frequency to the corresponding optical modes. It has recently been successfully demonstrated and results in low phase noise RF beatnotes with the linewidth in near hertz level.<sup>23</sup>

### 3.3 Mode-Crossing Effects on Kerr Combs

In an ultrahigh  $Q$  resonator coupled with a fiber taper, very complicated mode structures can be easily observed. Here, we put the taper in contact with the resonator to further excite higher-order modes and increase the mode-crossing

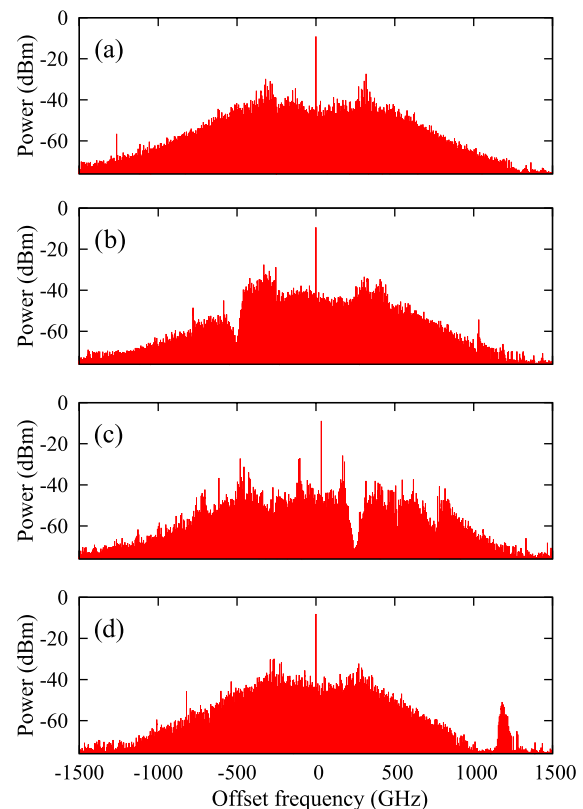


**Fig. 4** Spectra of symmetric and asymmetric Kerr frequency combs with single-FSR spacing when arbitrary WGMs are pumped.



probability. Figure 4 presents a Kerr comb spectra obtained when arbitrary modes are pumped. In comparison, a symmetric comb spectrum is presented in Fig. 4(a). As can be seen, Figs. 4(b) and 4(c) show asymmetric combs with locally weakened comb lines in either smaller or larger frequency regimes within 500 GHz offset from the pump. The enhanced comb lines are also observed in Fig. 4(d). These effects could result from the mode-crossing and possibly higher-order dispersion.<sup>19,42</sup> The small spectra spanning range could result from the high-order mode excitation and low coupling efficiency.

#### 4 Conclusion

In conclusion, we have shown that a generation of primary combs with line spacings ranging from gigahertz to terahertz in a single resonator is possible. It is known that it is generally difficult to obtain primary combs with low multiple-FSR spacing ( $<10$ ). The present work thereby proves that combs with a stable frequency spacing of 24 GHz can be generated, thereby allowing the achievement of ultrastable microwave generation in frequency bands of interest for aerospace technology. We have also presented experimental evidence of thermal locking effects on various families of modes, as well as the asymmetric combs that arise from a mode-crossing effect in an overmoded resonator. Future work would include a necessary pump-resonance locking technique to avoid thermal noises and better study of Kerr combs for low phase noise microwave generation.

#### Acknowledgments

The authors acknowledge financial support from the European Research Council through the project NextPhase (ERC StG 278616). They also acknowledge financial support from the *Centre National d'Etudes Spatiales* through the project SHYRO (Action R & T-R-S10/LN-0001-004/DA:10076201), and from the *Région de Franche-Comté*.

#### References

1. T. Kippenberg, S. Spillane, and K. Vahala, "Kerr-nonlinearity optical parametric oscillation in an ultrahigh-Q toroid microcavity," *Phys. Rev. Lett.* **93**(8), 083904 (2004).
2. A. A. Savchenkov et al., "Low threshold optical oscillations in a whispering gallery mode CaF<sub>2</sub> resonator," *Phys. Rev. Lett.* **93**(24), 243905 (2004).
3. P. Del'Haye et al., "Optical frequency comb generation from a monolithic microresonator," *Nature* **450**(7173), 1214–1217 (2007).
4. P. Del'Haye et al., "Frequency comb assisted diode laser spectroscopy for measurement of microcavity dispersion," *Nat. Photonics* **3**(9), 529–533 (2009).
5. P. Del'Haye, S. B. Papp, and S. A. Diddams, "Hybrid electro-optically modulated microcombs," *Phys. Rev. Lett.* **109**, 263901 (2012).
6. S. B. Papp, P. Del'Haye, and S. A. Diddams, "Mechanical control of a microrod-resonator optical frequency comb," *Phys. Rev. X* **3**, 031003 (2013).
7. P. Del'Haye et al., "Self-injection locking and phase-locked states in microresonator-based optical frequency combs," *Phys. Rev. Lett.* **112**, 043905 (2014).
8. J. Li et al., "Low-pump-power, low-phase-noise, and microwave to millimeter-wave repetition rate operation in microcombs," *Phys. Rev. Lett.* **109**, 233901 (2012).
9. L. Razzari et al., "CMOS-compatible integrated optical hyper-parametric oscillator," *Nat. Photonics* **4**(1), 41–45 (2010).
10. J. S. Levy et al., "CMOS-compatible multiple-wavelength oscillator for on-chip optical interconnects," *Nat. Photonics* **4**(1), 37–40 (2010).
11. F. Ferdous et al., "Spectral line-by-line pulse shaping of on-chip microresonator frequency combs," *Nat. Photonics* **5**(12), 770–776 (2011).
12. T. Herr et al., "Universal formation dynamics and noise of Kerr-frequency combs in microresonators," *Nat. Photonics* **6**(7), 480–487 (2012).
13. J. Pfeifle et al., "Microresonator-based optical frequency combs for high-bitrate WDM data transmission," presented at *Optical Fiber Communication Conf.*, Optical Society of America, Los Angeles, OW1C.4 (4–8 March 2012).
14. P.-H. Wang et al., "Observation of correlation between route to formation, coherence, noise, and communication performance of Kerr combs," *Opt. Express* **20**(28), 29284–29295 (2012).
15. K. Saha et al., "Modelocking and femtosecond pulse generation in chip-based frequency combs," *Opt. Express* **21**(1), 1335–1343 (2013).
16. H. Jung et al., "Optical frequency comb generation from aluminum nitride microring resonator," *Opt. Lett.* **38**(15), 2810–2813 (2013).
17. W. Liang et al., "Generation of near-infrared frequency combs from a MgF<sub>2</sub> whispering gallery mode resonator," *Opt. Lett.* **36**(12), 2290–2292 (2011).
18. I. S. Grudinin, L. Baumgartel, and N. Yu, "Frequency comb from a microresonator with engineered spectrum," *Opt. Express* **20**(6), 6604–6609 (2012).
19. T. Herr et al., "Mode spectrum and temporal soliton formation in optical microresonators," arXiv preprint arXiv:1311.1716 (2013).
20. A. A. Savchenkov et al., "Stabilization of a Kerr frequency comb oscillator," *Opt. Lett.* **38**(15), 2636–2639 (2013).
21. A. Coillet and Y. K. Chembo, "On phase-locking of Kerr combs," arXiv preprint arXiv:1401.0930 (2014).
22. T. Herr et al., "Temporal solitons in optical microresonators," *Nat. Photonics* **8**(2), 145–152 (2014).
23. A. A. Savchenkov et al., "Tunable optical frequency comb with a crystalline whispering gallery mode resonator," *Phys. Rev. Lett.* **101**, 093902 (2008).
24. I. S. Grudinin, N. Yu, and L. Maleki, "Generation of optical frequency combs with a CaF<sub>2</sub> resonator," *Opt. Lett.* **34**(7), 878–880 (2009).
25. A. Savchenkov et al., "Kerr combs with selectable central frequency," *Nat. Photonics* **5**(5), 293–296 (2011).
26. A. A. Savchenkov et al., "Kerr frequency comb generation in overmoded resonators," *Opt. Express* **20**(24), 27290–27298 (2012).
27. Y. K. Chembo, D. V. Strekalov, and N. Yu, "Spectrum and dynamics of optical frequency combs generated with monolithic whispering gallery mode resonators," *Phys. Rev. Lett.* **104**, 103902 (2010).
28. Y. K. Chembo and N. Yu, "Modal expansion approach to optical-frequency-comb generation with monolithic whispering-gallery-mode resonators," *Phys. Rev. A* **82**, 033801 (2010).
29. A. B. Matsko et al., "Mode-locked Kerr frequency combs," *Opt. Lett.* **36**(15), 2845–2847 (2011).
30. Y. K. Chembo and C. R. Menyuk, "Spatiotemporal Lugiato-Lefever formalism for Kerr-comb generation in whispering-gallery-mode resonators," *Phys. Rev. A* **87**, 053852 (2013).
31. S. Coen et al., "Modeling of octave-spanning Kerr frequency combs using a generalized mean-field Lugiato-Lefever model," *Opt. Lett.* **38**, 37–39 (2013).
32. A. Coillet et al., "Azimuthal Turing patterns, bright and dark cavity solitons in Kerr combs generated with whispering-gallery-mode resonators," *IEEE Photon. J.* **5**, 6100409 (2013).
33. C. Godey et al., "Stability analysis of the Lugiato-Lefever model for Kerr optical frequency combs. Part I: case of normal dispersion," arXiv preprint arXiv:1308.2539 (2013).
34. I. Balakireva et al., "Stability analysis of the Lugiato-Lefever model for Kerr optical frequency combs. Part II: case of anomalous dispersion," arXiv preprint arXiv:1308.2542 (2013).
35. A. Rolland et al., "Non-linear optoelectronic phase-locked loop for stabilization of opto-millimeter waves: towards a narrow linewidth tunable THz source," *Opt. Express* **19**(19), 17944–17950 (2011).
36. A. A. Savchenkov et al., "Phase noise of whispering gallery photonic hyper-parametric microwave oscillators," *Opt. Express* **16**(6), 4130–4144 (2008).
37. A. B. Matsko et al., "Chaotic dynamics of frequency combs generated with continuously pumped nonlinear microresonators," *Opt. Lett.* **38**, 525–527 (2013).
38. A. Coillet and Y. K. Chembo, "Routes to spatiotemporal chaos in Kerr optical frequency combs," *Chaos* **24**(1), 013113 (2014).
39. T. Carmon, L. Yang, and K. Vahala, "Dynamical thermal behavior and thermal self-stability of microcavities," *Opt. Express* **12**(20), 4742–4750 (2004).
40. G. Lin et al., "Thermal bistability-based method for real-time optimization of ultralow-threshold whispering gallery mode microlasers," *Opt. Lett.* **37**(24), 5193–5195 (2012).
41. A. A. Savchenkov et al., "Morphology-dependent photonic circuit elements," *Opt. Lett.* **31**(9), 1313–1315 (2006).
42. I. S. Grudinin, L. Baumgartel, and N. Yu, "Impact of cavity spectrum on span in microresonator frequency combs," *Opt. Express* **21**(22), 26929–26935 (2013).

**Guoping Lin** received his joint PhD degrees in optics and physics from Xiamen University, China, and from École Normale Supérieure of Paris, France, in 2010. From 2011 to 2013, he was a NASA postdoctoral program fellow at the Jet Propulsion Laboratory, Pasadena. He is now a postdoctoral fellow at FEMTO-ST Institute in Besançon, France, where he is working on miniature spectrally pure microwave sources based on ultrahigh-Q crystalline optical resonators.

**Khaldoun Saleh** received his MSc degree in 2009 and his PhD degree in 2012, both in microwaves, electromagnetism, and optoelectronics from the Toulouse III University, Toulouse, France. Since 2013, he has been a postdoctoral fellow at FEMTO-ST Institute, where he is working on the improvement of high spectral purity microwave sources based on whispering gallery mode resonators.

**Rémi Henriet** received his MSc degree in physics from the University of Franche-Comté, France, in 2011. In 2011, he started his PhD on the topic of opto-electronic oscillators based on ultrahigh- $Q$  whispering-gallery mode resonators at FEMTO-ST Institute in Besançon, France.

**Souleymane Diallo** received his MSc degree in physics from the University of Franche-Comté, France, in 2013. In 2013, he started his PhD on the topic of optimization of Kerr frequency combs in whispering gallery mode resonators at FEMTO-ST Institute in Besançon, France.

**Romain Martinenghi** received his MSc degree in physics in 2010 and his PhD degree in optics and photonics in 2013, from the University of Franche-Comté, France. Since 2014, he has been a postdoctoral

fellow at FEMTO-ST Institute, France, where he is working on the development of high spectral purity microwave photonic oscillator and microwave electronics.

**Aurélien Coillet** received his MSc in physics from *École Normale Supérieure* of Lyon, France, in 2008. In 2011, he received his PhD in nonlinear optics from *Laboratoire Interdisciplinaire Carnot de Bourgogne*, Dijon, France. From 2012 to 2014, he was a postdoctoral fellow at FEMTO-ST Institute, Besançon, France. He is now a postdoctoral fellow at National Institute for Standards and Technology, Boulder. His research is focused on optoelectronics, nonlinear optics, and nonlinear dynamics.

**Yanne K. Chembo** received a PhD in physics in 2005 from the University of Yaoundé I, Cameroon, a PhD in laser physics in 2006 from the University of the Balearic Islands, Spain, and a Habilitation degree in 2011 from the University of Franche-Comté, France. In 2009, he was a NASA postdoctoral program fellow at the Jet Propulsion Laboratory, Pasadena. Since 2010, he has been a senior research scientist at *Centre National de la Recherche Scientifique*.